

Pilot-scale multi-stage reverse osmosis (DT-RO) for water recovery from landfill leachate

D., Cingolani^{1,*}, F. Fatone¹, N. Frison², M., Spinelli¹, A.L., Eusebi¹

¹ Department of Science and Engineering of Materials, Environment and Urban Planning (SIMAU), Università Politecnica delle Marche, Via Brecce Bianche, 12, Ancona, Italy.

*d.cingolani@univpm.it

² Department of Biotechnology, University of Verona, Via Le Grazie 15, 37134, Verona, Italy.

Abstract: Recovery of high quality water from municipal landfill leachate was studied by three-stage disc tube reverse osmosis optimized in pilot-scale. Following UF-membrane-assisted activated sludge plant, overall 46.5 tons of leachate were post-treated in real environment and analyzed for conventional contaminants and hazardous compounds (e.g. heavy metals, boron, selenium) throughout operation of membrane system.

Operating pressure ranged from 21 to 76 bar, while permeate flux varied in the range 7.1-32.5 L m⁻² h⁻¹. Rejection factors of specific ions were related to the pressure and global removals were assessed for each stage (e.g. E%_{COD} = 92.4-99.2%, E%_{NH₄} = 46.2-95.8%, E%_{NO_x} = 84.8-97.9%; E%_{TDS} 88-95.5%). Boron removal was assessed in the range 34-48%, so as to require the third stage to reach standard for discharge or reuse. Two stages were sufficient to reach water recovery higher than 91%. Long-term operation and mathematical modeling demonstrated how the $\Delta\pi/\Delta P$ ratio can support the decisions for membrane cleaning and predictive maintenance: permeability decline was associated to the ratio increase from 0.72-0.73 to 1.13-1.21.

Keywords: reverse osmosis operation; landfill leachate; water recovery; boron rejection; DT-RO.

27	Nomenclature	
28	μ	Dynamic viscosity
29	A	Membrane permeability
30	ABS	Acrylonitrile Butadiene Styrene
31	COD	Chemical Oxygen Demand
32	CP	Concentration Polarization
33	CV	Coefficient of Variation
34	DT-RO	Disc Tube Reverse Osmosis
35	E%	Efficiency removal
36	ERS	Energy Recovery System
37	FP	Booster pump
38	J_w	Permeate flux
39	k	Electrical conductivity
40	MBR	Membrane Biological Reactor
41	MF	Micro filter
42	MSW	Municipal solid waste
43	MWWTP	Municipal Wastewater Treatment Plant
44	PA	Polyamide
45	PLC	Programmable Logic Controller
46	P_{max}	Set-point of maximum pressure
47	PP	Piston pump
48	Q_c	Concentrate flow rate
49	Q_p	Permeate flow rate
50	R	Rejection factor
51	RO	Reverse Osmosis
52	RO1	RO stage one

53	RO2	RO stage two
54	RO3	RO stage three
55	RR%	Recovery rate
56	SEC	Specific Energy Consumption
57	SW	Spiral wound
58	T	Temperature
59	TDS	Total Dissolved Solids
60	TFC	Thin Film Composite
61	TKN	Kjeldahl Nitrogen
62	UF	Ultrafiltration
63	VC	Concentrate spillage valve
64	WWTP	Wastewater Treatment Plant
65	ΔP	Operative pressure differential
66	$\Delta \pi$	Osmotic pressure differential
67	π	Osmotic pressure

68 **1. Introduction**

69 Landfilling is still a major issue of the municipal solid waste management system in Europe
70 and, even more, around the world. In 2015, 61 Mtons of municipal solid waste (MSW) have
71 been landfilled in Europe while the generated leachate may be estimated between 12.2 and 61
72 Mtons (Brennan et al., 2016; Eurostat, 2015). This residual must be appropriately treated and
73 managed, maximizing the recovery and minimizing the waste disposals. In particular,
74 standalone on-site treatments are more and more attractive to cope with the changing and
75 variable characteristics of leachate (Brennan et al., 2016). In this context, the use of membrane
76 technologies allows stable quality of the permeate that can be locally reused or discharged in
77 water bodies (Hasar et al., 2009). In particular, Reverse Osmosis (RO), either as a main step in
78 a landfill leachate treatment chain or as single post-treatment step has shown to be an
79 indispensable means of achieving high purification, removal of hazardous metals and potential
80 water recovery (Ahmed and Lan, 2012; Renou et al., 2008). However, the specific energy
81 consumption (SEC) of RO is much higher than other treatments. Judd (2017) highlighted that
82 multi-stage RO improves water recovery and reduces SEC when less than five stages are used.
83 Feasibility and sustainability of RO system depends on the brine disposal. One of the most
84 viable and practiced way is the reinjection (or recirculation) of the brine into the landfill.
85 Generally, 30% of the volume of the raw leachate is returned to the landfill as concentrated
86 stream (Li et al., 2009). Few scientific papers debate on this topic and opinions to such practices
87 are conflicting (Calabrò et al., 2010; Peters, 1998). This operation will always return salinity
88 and contaminants into the landfill resulting in increasing in osmotic pressure for leachate
89 separation and higher SEC for the RO plant.

90 By avoiding the recirculation of the concentrate in the landfill, the viability of the on-site
91 treatment of the leachate and discharge into the surface water bodies require a high energy
92 consumption, up to an expensive of 30 €/m³ of influent flow.

93 In desalination processes, costs related to thermal treatment and brine disposal may rise until
94 33% of the total cost of desalination (Pérez-González et al., 2012). Thus, the cost-related to the
95 concentrate disposal in the separation of the landfill leachate might be much higher.

96 Since the feasibility and sustainability of RO is usually limited by the disposal of the
97 concentrate, its minimization is the first strategy to make the treatment sustainable.

98 The performances of RO can be optimized coupling two or more stages. This configuration
99 minimizes the concentrate and maximizes the water recovery (Joo and Tansel, 2015; Subramani
100 and Jacangelo, 2014), being able to achieve high removal of persistent anion like boron (Hilal
101 et al., 2011).

102 However, although hybrid or conventional technologies have been developed trying to be
103 economically attractive (Cingolani et al., 2017; Mukherjee et al., 2015), the technical and
104 economic sustainability of RO multi-stage scheme is limited by membrane fouling (Bourgeois
105 et al., 2001; Zhao et al., 2013). Disc tube RO (DT-RO) technology has widely been proposed
106 for on-site landfill leachate, particularly for high suspended solid matrices (Gong et al., 2013;
107 Hasar et al., 2009; Insel et al., 2013; Smol and Włodarczyk-Makuła, 2016; Zhang et al., 2013).

108 Compared to the conventional spiral wound (SW), tubular or hollow fibre modules, the “plate-
109 and-frame” configuration of the DT module and the shorter flow path (≈ 7.5 cm) guarantees
110 higher turbulence and limits the concentration polarization (CP) effects along the surface of the
111 membrane (Peters, 2001; Singh, 2015; Subramani and Jacangelo, 2014). Nevertheless,
112 concentrate production and fouling rates in real environment are still gaps of knowledge.

113 Therefore, the paper demonstrates how the optimization of water recovery and removal of
114 nitrate, boron and selenium from pre-treated landfill leachate, up to reuse or discharge quality
115 standard, need a triple-stage DT-RO scheme.

116 The plant was then studied in terms of operational viability and to compare performances with
117 single stage RO, that was able to achieve the required effluent standard.

118 Three RO stages were studied to maximize the water recovery in the first two (Alghoul et al.,
119 2009), while the third was investigated to achieve high quality permeate. As the pilot plant was
120 installed in full-scale field, attention was paid to the relevant, unpredictable and sudden
121 variability of influent that can drastically influence permeability, recovery rates and permeate
122 quality.

123 Finally, removal of persistent ions such as boron and selenium was investigated to define
124 suitable configuration to achieve standard for reuse or discharge in sensitive water bodies.

125

126 **2. Material and methods**

127 The multi-stage RO was operated for three relevant months to treat the effluent of a full-scale
128 plant (Marche Region, Italy) that is treating municipal landfill leachate with treatment capacity
129 of 300 m³/d. Before the RO, hereby focused, the leachate is pre-treated by clari-flocculation,
130 activated sludge with intermittent aeration and tertiary membrane ultrafiltration (Eusebi et al.,
131 2009). The plant has already been monitored for one year by defining the characteristics of
132 influent and effluent: results have been published in a previous work (Cingolani et al., 2017).

133 The raw leachate is originated from two nearby MSW landfills serving a basin of 460,000
134 inhabitants in Marche Region (central Italy). The overall treatment capacity of 115,800 ton of
135 MSW per year is divided between a 44-ha site operating since 1989 and a 11.4-ha operating
136 since 1999 (ARPAM, 2016).

137

138 **2.1 The DT-RO pilot plant**

139 The RO pilot-scale plant was equipped with DT modules (Figure 1-a). The membranes (Gel
140 GPT-BW 30) were installed into the stainless-steel vessel of 1.2 m length (Figure 1-a).
141 Supporting discs were made in acrylonitrile butadiene styrene (ABS) with an outer diameter of
142 197 mm. Every overlapped disc (Figure 1-a) contains two films of polyamide (PA) thin-film-
143 composite (TFC) with the following specifications: NaCl rejection >98%, max pressure 120

144 bar, max temperature 40°C, pH operating 3-11, free chlorine tolerance <0.1 ppm. The whole
145 membrane area was of 7.7 m².

146 Inlet feeding was provided through one booster (FP) and one piston (PP) pump (Figure 1-b).

147 The feeding inter-crosses the disc package from the bottom to the top. The pressure-driven
148 process directs the permeate towards the central channel of the vessel (Figure 1-a), besides the
149 concentrate continuously crosses the package to be sent to the feed outlet pipe.

150 Chemical conditioning of the feeding was provided by the dosage of sulfuric acid (30% w/w)
151 through the control of pH-meter (Georg Fischer, electrode model 3-2724-01).

152 Electrical conductivity (*k*) measurements were performed both for feeding and permeate
153 streams (EMEC, models ECDC/1 and ECDCC/10), the temperature was monitored in the
154 feeding pipe (IFM model TA2435). Inlet and outlet pressures were continuously monitored
155 (Siemens SITRANS P220) and flow rates were measured for the permeate (Q_p) and the
156 concentrate (Q_c) (IFM model SM6100).

157

158 **2.2 Reverse osmosis plant and operative process parameters**

159 The RO was organized in consecutive phases (Figure 2). RO1 treated the effluent from the full-
160 scale membrane bioreactor. The concentrate from RO1 was reduced by RO2 stage at high
161 pressure and the last refinement stage RO3 treated the mixed permeate from RO1 and RO2.

162 Table 1 shows the operating values for the permeate flow rate (Q_p) in each stage.

163 According to Hasar et al. (2009) and Linde et al. (1995), permeate flux (J_w) was set to 13 L m⁻²
164 h⁻¹ in the first RO1. Due to the concentration of the inlet, J_w was decreased up to 7.1 L m⁻² h⁻¹
165 in the RO2. Finally, J_w was set to 32.5 L m⁻² h⁻¹ in the refinement stage RO3.

166 With the purpose to maintain the recovery rate (RR%) stable, concentrate production (Q_c) was
167 consequently managed by recirculating in the feeding tank or spilling (Figure 1-b).

168 The programmable logic controller (PLC) automatically adjusted the operating pressure to keep
169 the permeate flux constant until the maximum set pressure value (P_{\max} - Table 1). J_w of 2 L m^{-2}
170 h^{-1} was chosen as setpoint to stop the test.

171 Sulfuric acid was dosed to maintain the pH of 6.5 in the RO1 trials. All set of runs were
172 performed in the range 29.1 to 37.9 °C.

173

174 **2.3 Analytical methods and process model**

175 Membrane fouling phenomena can be investigated by monitoring the water permeability (Kim
176 and Hoek, 2005). To monitor the decline of membrane permeability the following assumptions
177 were made: (1) the membrane package was considered as a single layer, (2) ΔP is averaged
178 between inlet and outlet, (3) $\Delta\pi$ is assumed as bulk osmotic pressure differential.

179 The permeability was normalized at 25°C according to Equation 1 (Eq.1) (Sassi and Mujtaba,
180 2012), where μ is the dynamic viscosity of feeding:

$$181 \quad A^T = A^{T_0} \frac{\mu^{T_0}}{\mu^T} \quad (\text{Eq.1})$$

182 During the experimental phase the pilot plant was operated 24 hours per day. Samples of pre-
183 treated ultra-filtered leachate (UF leachate) were daily collected. Differently, samples of the
184 ROs streams (feeding, permeate and concentrate) were collected 3 times per day every 4 hours
185 separately for RO1, RO2 and RO3, then stored at 4°C and analysed within 12-24 hours.

186 Analytical study was executed for the main conventional pollutants (COD, ammonia and TKN)
187 according to standard methods (APHA, 2005). pH was measured using a Metrohm 848 titrator
188 and alkalinity was determined through titration via chloridric acid. Electrical conductivity (k)
189 was performed by an XS Cond 70. Ion concentrations (NO_2^- , NO_3^- , PO_4^- , Cl^- , SO_4^- , Na^+ , K^+ ,
190 Mg^{++} , and Ca^{++}) were measured using ion chromatograph (IC) (Dionex, DX-120 equipped with
191 IonPac AS9-HC column, ICS-1000 equipped with IonPac CS12A column).

192 Total metals and non-metals concentrations were determined by inductively coupled plasma
193 mass spectrometry (ICP-MS) (Perkin Elmer model Optima 8300). ICP-MS analysis was

194 performed on composite samples only on the streams of UF leachate, permeate of RO1,
195 permeate of RO3 and residual concentrate from RO2 previously acidified to a pH of less than
196 2 with nitric acid.

197 The osmotic pressure was monitored by relating k and π : online values of π and temperature
198 were used to predict the permeability of the membrane package in each stage.

199 Leachate strength and process performances were mainly evaluated by the removal of salt
200 content. Rejection factors (R) were calculated according to Equation 2 (Eq. 2).

$$201 \quad R (\%) = \left(1 - \frac{C_p}{C_i}\right) \times 100 \quad (\text{Eq. 2})$$

202 where C_p (mg/L) and C_i (mg/L) are the ion concentrations in the permeate and the
203 corresponding feeding streams, respectively.

204 On the other hand, the removal efficiency (E) was calculated on mass balances basis.

205 Recovery rate (RR%) was calculated as the ratio of the volume permeated with respect to the
206 volume treated. Membrane cleaning was carried out at the beginning of each stage by
207 alternating water flushing and chemical washings. Acid (citric acid 2% w/w, lactic acid 0.5%
208 w/w, dodecylbenzenesulfonic acid 0.5% w/w) and basic cleaners (KOH 4% w/w and Na₄EDTA
209 0.5% w/w) were used.

210

211 **3. Results and Discussion**

212 **3.1 Operation of RO1**

213 The chemical and physical characterization of the UF leachate is reported in Table 2. Feeding
214 in the RO1 stages had a considerable amount of non-biodegradable organic carbon and high
215 salinity, mainly related to chlorides and sodium. Ammonia was in the range 35±46 mgNH₄-
216 N/L thanks to the secondary biological treatment. Differently, NO_x-N in the range 398±282
217 mgN/L were related to scarce biological denitrification.

218 Relevant variability of the UF leachate was observed along the experimental period that
219 included both dry and wet seasons.

220 The management of recycles and retentate in a multiple stage RO is a key strategy often
221 neglected in lab scale experiments. In this full-scale field study, the monitored parameters of
222 RO1_C run are shown in Figure 3 where Q_c was null at the beginning of the test. Pressure-driven
223 process was continuously concentrating the feeding due to the recirculation stream (Figure 1-
224 b), so the electrical conductivity of the inlet increased from 12 mS/cm up to 45 mS/cm. The
225 concentrate flow rate (Q_c) was pumped out from hour 45 onwards in order to stabilize electrical
226 conductivity in the influent. Therefore, k was manually adjusted at 35 mS/cm.

227 When the pressure set point (P_{max}) was reached, Q_p began to fluctuate from 80 to 100 L h⁻¹ due
228 to the concentrate flow adjustments and the changes of k in the feed.

229 After 100 hours, fouling led the permeate flux decline from 13 to 6.8 L m⁻² h⁻¹ (corresponding
230 to Q_p decline from 100 to 52.5 L h⁻¹, Figure 3). Then, the permeability A^{T_0} was recovered at
231 1.13 L m⁻² h⁻¹ bar⁻¹ thanks to chemical cleaning.

232 TFC-PA membranes from the biggest manufacturers in the world have a normalized water
233 permeability from 0.8 to 8 (Lee et al., 2011) depending on salt rejections (NaCl) between 98%
234 and 99.8%. The actual permeability makes the membrane falling within the category of high
235 rejections and less production of permeate.

236 When the inlet pressure in RO1 runs ranged between 20 and 67 bar, the mean working
237 conditions were of 50.5, 33.4 and 47.7 bar for RO1_A, RO1_B and RO1_C, respectively. Major
238 effect on the overall pressure drop was found by the hydraulics of the membrane module. On
239 the other hand, membrane fouling did influence the permeate flowrate.

240 Figure 4 reports rejection of conventional pollutants in RO1: remarkably, ΔP influenced mainly
241 the rejection of ammonia and TDS. In run RO1_A, rejections of TDS (93-96%, Figure 4-a) and
242 ammonia (27.4-65.5%, Figure 4-b) increased from ΔP of 26 to 63 bar. Better rejection trends
243 were found for the B and C runs, where R_{NH_4} was between 73%-91% and ΔP ranged from 10.9
244 to 63.4 bar. Similar trend was observed for NO_x-N (Figure 4-c).

245 No clear correlation between ΔP and COD rejection was found (Figure 4-d), but two tendencies
246 can be clearly seen in the run B: both increase COD rejection as a function of pressure. Since
247 the temperature was of $34.3 \pm 2.4^\circ\text{C}$, $35.6 \pm 1.8^\circ\text{C}$, $35.5 \pm 2.6^\circ\text{C}$ respectively for A, B and C
248 runs, its effect on COD rejection has been excluded. The behavior has been related to an
249 intermediate stop and restart of the run, for approximately 2 days of break, where a rinsing with
250 water was executed.

251 COD removal between 95% and 99% was observed as reported also by other authors (Kuusik
252 et al., 2014; Talalaj, 2015) as well as rejection factors related to pressure drops (Singh, 2015).
253 However, increase of rejection rates were observed from run A to run B and C and were
254 associated to the irreversible fouling and water permeability decline (Bellona et al., 2004).

255

256 **3.2 Operation of RO2 and RO3**

257 The conductivity in the feed of RO2 stages was 18.6 mS/cm in run A, 60.3 mS/cm in B and
258 36.9 mS/cm in C. These values are indirect indicators of COD and TDS that were: 2,335
259 mgCOD/L and 15.6 gTDS/L for RO2_A; 13,512 mgCOD/L and 57.3 gTDS/L for RO2_B; 7,352
260 mg/L mgCOD/L and 34.5 gTDS/L for RO2_C.

261 Contrary to the RO1 stages, the high pressure (RO2) and refinement (RO3) ones were executed
262 without withdrawing the concentrate (Figure 1-b). This approach led to the continuous increase
263 of feeding π and operative pressure that influenced the fouling rate.

264 In the RO2_A, inlet pressure increased from 15 to 35 bar and the permeate flux was kept to 6.4
265 $\text{L m}^{-2} \text{h}^{-1}$. Differently, in the cases of RO2_{B-C} the starting pressures were of 60 and 40 bar
266 respectively, due to higher salinity of feeding. After that pressure raised up to P_{\max} , J_w was
267 rapidly decreasing from 6.4 to 2 $\text{L m}^{-2} \text{h}^{-1}$ until the runs were stopped. Average values of inlet
268 pressure are reported in Table 3. The lower pressure in RO2_A than RO2_{B-C} was linked both to
269 the low salinity and to the set operative flux of permeate (half to the RO1 one).

270 Rejection factors into the RO2 stages were found as function of pressure likely the RO1 ones,
271 R_{TDS} changed from 88% to 94% at 16 and 30 bar respectively in the RO2_A case, while it was
272 from 95% to 98% at 40 bar and 97 bar in the others RO2_{B-C} runs.

273 Besides, worsening rejection of TDS was noticed when the permeate flux was decreasing. R_{TDS}
274 of 92% were recorded at the end of RO2_C due to highest $\Delta\pi$. Rise of salt passage was related to
275 an increase of CP to the permeate side due to flux decline (Agenson and Urase, 2007; Wijmans
276 and Baker, 1995).

277 Combination of permeates originated from RO1 and RO2 stages were characterized by 53 ± 26
278 mg COD/L, 13.2 ± 6.7 mg NH₄-N/L, 94 ± 60 mg NO_x-N/L, 203 ± 81 mgCl⁻/L and 206 ± 49
279 mgNa⁺/L. Accordingly, the electrical conductivity of feeding in RO3 runs was of 1.28 and 1.69
280 mS/cm respectively for A and B series.

281 During the RO3 stages, the assigned permeate flow rate of 250 L h⁻¹ was kept constant over all
282 the testing period. RO3_A continuously worked at 23.4 ± 1.2 bar of inlet pressure, while RO3_B
283 started from 40 bar up to reach 63 bar (average pressure of 41.8 ± 4.5 bar). Both RO3 runs were
284 performed until achieving the feeding concentration factor up to 10 times.

285 Inconsistently operative pressures among RO3 stages have been linked to membrane condition,
286 as stated by permeability that decreased from 1.5 to 0.8 L m⁻² h⁻¹ bar⁻¹.

287

288 **3.3 Recovery rates and permeate quality**

289 RO1 and RO2 played a major role in the water recovery (Figure 2). However, the recovery was
290 relatively high (>90%) even in the third stage.

291 Depending on the quality of the UF leachate, recovery rates (RR%) ranged from 66% to 87%
292 in the three RO1 runs, where the feeding k varied between 11.1 ± 0.7 mS/cm and 6.2 ± 0.9
293 mS/cm.

294 Differently, the RR% in RO2 increased from 34% (Feeding $k = 60.3$ mS/cm) up to 72%
295 (Feeding $k = 18.6$ mS/cm), confirming the relation between the recovery rate and the initial

296 electrical conductivity. Therefore, global RR% of the multi-stage filtration was observed in a
297 range of 91-95%.

298 Few literature papers report water recovery data for similar applications on landfill leachate, as
299 they commonly refer to the brackish water (BW) desalination (with TDS concentration between
300 1,000-15,000 mg/L). The design practice usually leads to a global recovery of 82%: 64% in the
301 first stage and 50% in the second one (Alghoul et al., 2009).

302 Altaee and Hilal (2015) proposed a hybrid multi-stage membrane treatment (NF-FO/BWRO)
303 to produce fresh water for humans and agriculture. NF recovery was from 50% to 75% at feed
304 salinity from 1 g/L to 2.4 g/L, while FO-BWRO could recover only 18%. Linde et al. (1995)
305 reported recovery between 51-71% for the first RO stage in landfill leachate desalination.
306 Where feeding k was in the range 1.5-2.5 mS/cm, pressure was assessed of 30-40 bar.

307 The quality of permeate from each RO stage is shown in Table 2, while heavy metal
308 concentrations of the main streams are reported in Table 4. Except for NO₂-N and NO₃-N, RO1
309 allowed to reach the standard for discharge in sensitive water bodies. However, water recovery
310 can be optimized to more than 90% only by following RO2 and RO3 stages.

311 Rejection factors are influenced by the inlet pressure as well as removal efficiencies (Table 3).
312 Metals concentrations reached standard for discharge already after RO1. Selenium removal was
313 higher than 94% while boron removal was assessed in the range 34-48%. As result, the full
314 three-stage configuration was necessary to decrease boron in the permeate below 2 mg/L and
315 achieve the standard for reuse. However, it must be noticed the high B concentration in the
316 concentrate that must be incinerated or crystallized, leading to high overall treatment costs.

317 Al, Fe and Cd concentrations in the permeate of RO3 were higher than RO1. As the refinement
318 RO3 treated also the permeate of RO2 (Figure 2), the increase in RO3 effluent could be related
319 to higher influent loading. However, no analytical evidence can support this comment.

320 These results are comparable with Smol and Włodarczyk-Makuła (2016) that studied an
321 integrated system of coagulation-NF/RO. Lower performance on COD removal (59%) was

322 reported by Ahn et al. (2002) by using SWRO PA membranes (Filmtec) to study an MBR-RO
323 configuration to treat landfill leachate in full-scale.

324

325 **3.4 Modeling membrane permeability and fouling rates**

326 The model was calibrated to obtain π values and was used to evaluate $\Delta\pi$ that were determined
327 according to the following quadratic equation.

$$328 \quad \pi(T) = (a(T) \cdot k^T + b(T))^2 \quad (\text{Eq. 3})$$

329 where k^T is the electrical conductivity at the operating temperature, $a(T)$ and $b(T)$ are the
330 experimental coefficients corresponding to the specific temperature. The calibration of the
331 model is reported in Figure 5. The fouling effect on permeability in the RO1 trials can be
332 recognized in Figure 6.

333 In run RO1_B, the initial permeability was $1.4 \text{ L m}^{-2} \text{ h}^{-1} \text{ bar}^{-1}$, after 150 hours without intermediate
334 cleanings it dropped down to $0.39 \text{ L m}^{-2} \text{ h}^{-1} \text{ bar}^{-1}$. At the same test conditions, in the RO1_C the
335 permeability of $0.4 \text{ L m}^{-2} \text{ h}^{-1} \text{ bar}^{-1}$ was reached in about 75 hours from the start of the test and
336 the initial permeability was lower than $1 \text{ L m}^{-2} \text{ h}^{-1} \text{ bar}^{-1}$. Notwithstanding the manufacturer's
337 recommended chemical cleanings, the initial permeability (A) was not recovered and the
338 fouling rate was higher (15.6×10^{-3} vs $6.5 \times 10^{-3} \text{ L m}^{-2} \text{ h}^{-2} \text{ bar}^{-1}$) (Figure 6). This demonstrates
339 the need of stronger and intermediate chemical cleaning.

340 In a full-scale DT-RO application treating raw leachate (Liu et al. 2008), alternating alkaline
341 cleaning every 100 h and acidic cleaning every 500 h Authors were able to recover 99% of the
342 initial permeability. Gong et al. (2013) in application of DT-RO for concentrating anaerobic
343 digestate (75% recovery and feeding $k = 22 \text{ mS/cm}$) stated the same result. Although they did
344 not report information about permeability decline, the fouling rate has been estimated to be $6 \times$
345 $10^{-4} \text{ L m}^{-2} \text{ h}^{-2} \text{ bar}^{-1}$, whereas the permeate flux was $12 \text{ L m}^{-2} \text{ h}^{-1}$. As result, the accurate control
346 on chemical cleaning ensured the longevity of the membrane.

347 Furthermore, the linear relationship among modeled data of $\Delta\pi$ (Eq. 3) with the pressure (ΔP)
348 was found (Figure 5, Figure 7) and is expressed by the following equation.

$$349 \quad \Delta\pi = c \Delta P - d \quad (\text{Eq. 4})$$

350 The slope value (c) is the fouling rate while the intercept with the y-axis (d) is the initial
351 operative pressure. Both parameters show preliminary information about the initial condition
352 of the membrane system. Therefore, the whole permeability could be assumed as function of
353 the pressure drop (ΔP), according to the Equation 5:

$$354 \quad A = \frac{J_w}{\Delta P + (1-c)d} \quad (\text{Eq. 5})$$

355 Ideally, c and d must be the same for similar hydrodynamics conditions, cleaning state and same
356 effects of internal and external concentration of polarization. Practically, both the coefficients
357 are influenced by piping configuration and membrane modules

358 As stated by Eq. 5, the permeability (A) decreases by raising d or decreasing c when the other
359 values are assumed constant.

360 When pressure increases the slope of the curve decreases (c parameter decreases - highlighted
361 zone in Figure 5). In particular, from hour 130 on in run RO1_B the correlation between ΔP and
362 $\Delta\pi$ is not linear, although the permeate flux remains at $13 \text{ L m}^{-2} \text{ h}^{-1}$, while ΔP increases from 40
363 to 67 bar. In the highlighted zone, the performances of the membrane decreased both for
364 permeability (Figure 6) and for the concentrations of the permeate. As consequence, $\Delta\pi$
365 decreases together with the rejection performances. In general, the fouling effects could be
366 linked to long filtration time, to cake layer formation, to extension and more compact of cake
367 layer impact and to internal and external polarization phenomena (Le and Nunes, 2016).
368 However, the contribution of each single phenomenon cannot be distinguished. Similar linear
369 trends have been observed also on the run C (Figure7).

370 Therefore, the analysis of $\Delta\pi/\Delta P$ could be used as indicator of the fouling rate and can be related
371 to the rejection parameters. In addition, the $\Delta\pi/\Delta P$ ratio can support the decisions for membrane
372 cleaning and predictive maintenance.

373

374 **3.5 DT-RO applicability and energy consumptions**

375 Comparing and assessing different RO membranes and modules geometry should consider both
376 performances and costs. Those include mainly energy consumption, chemicals, replacement
377 and initial investment.

378 In RO purification of landfill leachate with a conductivity of 15-16 mS/cm, Peters (1998) has
379 stated the time to replace the DT membranes as more than three years. Recovery rate around
380 80% and reinjection of concentrate into the landfill were adopted in that case.

381 Performances on concentrating landfill leachate by alternative RO systems are widely described
382 in literature papers. However, there is a gap of knowledge in assessing the optimal operating
383 parameters. Li et al. (2009) presented the RO treatment of landfill leachate ($k = 16$ mS/cm) in
384 tertiary treatment by using SW modules equipped by TFC membranes. Operating at average
385 flux of $6.5 \text{ L m}^{-2} \text{ h}^{-1}$ with a recovery of 53.4%, fouling rate was assessed to $1.8 \times 10^{-3} \text{ L m}^{-2} \text{ h}^{-2}$
386 bar^{-1} in a 90 hours cycle. Nonetheless, after 2 weeks of operation permeability was permanently
387 loss. In RO seawater desalination, SW membranes have an estimated lifespan of 2-5 years
388 (Avlonitis et al., 2003), in high salinity brackish water with high recovery rates the duration is
389 presumably shortened.

390 Among the available RO technologies, the cost for chemicals is almost uniform (0.28 to 0.33
391 €/m³). With regard to the capital cost, Vibratory Shear Enhanced Process (plate and frame RO
392 modules) has been considered representative for DT-RO CAPEX, equal to 34,900 €/ m³/h (75-
393 85% recovery) (Subramani and Jacangelo, 2014). Capital cost of the cheaper SWRO plant
394 ranges in 5,000-20,000 €/m³/h.

395 Lastly, the specific energy consumption of the pilot plant was in the range 15.8 to 20.9 kWh
396 per ton of treated leachate. However, the scale of the plant overestimate the SEC that has been
397 reported to be as high as 8.5 kWh/m³ in full scale DT-RO treatment plants (Rautenbach and
398 Linn, 1996) with 97% water recovery.

399

400 **4. Conclusion**

401 The triple-stage RO with DT technology has been studied as tertiary treatment for landfill
402 leachate in order to maximize water recovery and achieve the quality standard for discharge in
403 sensitive water bodies or water reuse.

404 The study has defined the membrane performances in terms of ions and metals rejection and
405 permeate quality of each single RO stage.

406 Rejection of the COD was higher than 95% and TDS removal was in the range 91.1% to 97.7%
407 when mean operating pressure was 33-76 bar. Rejection of ammonia ranged in the range 57.4-
408 77.3%.

409 By combining RO1 and RO2 the achieved recovery rate (RR%) was higher than 90%, but RO3
410 was necessary to achieve nitrogen and boron standards for discharge or reuse.

411 Drastic membrane and irreversible fouling was observed after 150 hours of continuous
412 filtration, and the $\Delta\pi/\Delta P$ ratio can support the decisions for membrane cleaning and predictive
413 maintenance. Prediction of fouling rates is feasible by measures of electrical conductivity and
414 ions concentrations.

415

416 **Acknowledgements**

417 This research was supported by the European Union through the Horizon2020 SMART-Plant
418 Innovation Action (grant agreement No 690323). Prof. Paolo Battistoni is gratefully
419 acknowledged for the inspiring discussion and suggestion for the process optimization. The
420 authors would like to thank GEL Spa for making the experimental equipment available and also

421 express their gratitude to Multiservizi Spa for its hospitality in the wastewater treatment plant.
422 The authors thank the reviewers for the constructive comments that helped to improve the
423 quality and potential impact of the paper.

424

425 **References**

- 426 Agenson, K.O., Uruse, T., 2007. Change in membrane performance due to organic fouling in
427 nanofiltration (NF)/reverse osmosis (RO) applications. *Sep. Purif. Technol.* 55, 147–156.
428 <https://doi.org/10.1016/j.seppur.2006.11.010>
- 429 Ahmed, F.N., Lan, C.Q., 2012. Treatment of landfill leachate using membrane bioreactors: A
430 review. *Desalination* 287, 41–54. <https://doi.org/10.1016/j.desal.2011.12.012>
- 431 Ahn, W.-Y., Kang, M.-S., Yim, S.-K., Choi, K.-H., 2002. Advanced landfill leachate
432 treatment using an integrated membrane process. *Desalination* 149, 109–114.
433 [https://doi.org/10.1016/S0011-9164\(02\)00740-3](https://doi.org/10.1016/S0011-9164(02)00740-3)
- 434 Alghoul, M.A., Poovanaesvaran, P., Sopian, K., Sulaiman, M.Y., 2009. Review of brackish
435 water reverse osmosis (BWRO) system designs. *Renew. Sustain. Energy Rev.*
436 <https://doi.org/10.1016/j.rser.2009.03.013>
- 437 Altaee, A., Hilal, N., 2015. High recovery rate NF–FO–RO hybrid system for inland brackish
438 water treatment. *Desalination* 363, 19–25. <https://doi.org/10.1016/j.desal.2014.12.017>
- 439 APHA, 2005. Standards methods for the examination of water and wastewater, 21th ed.
440 American Public Health Association, Washington D.C., USA.
- 441 ARPAM, 2016. Marche Region waste report.
442 http://www.arpa.marche.it/images/pdf/rifiuti/2016_Rapporto_rifiuti.pdf
- 443 Avlonitis, S.A., Kouroumbas, K., Vlachakis, N., 2003. Energy consumption and membrane
444 replacement cost for seawater RO desalination plants. *Desalination* 157, 151–158.
445 [https://doi.org/10.1016/S0011-9164\(03\)00395-3](https://doi.org/10.1016/S0011-9164(03)00395-3)

446 Bellona, C., Drewes, J.E., Xu, P., Amy, G., 2004. Factors affecting the rejection of organic
447 solutes during NF/RO treatment—a literature review. *Water Res.* 38, 2795–2809.
448 <https://doi.org/10.1016/j.watres.2004.03.034>

449 Bourgeois, K.N., Darby, J.L., Tchobanoglous, G., 2001. Ultrafiltration of wastewater: effects
450 of particles, mode of operation, and backwash effectiveness. *Water Res.* 35, 77–90.
451 [https://doi.org/10.1016/S0043-1354\(00\)00225-6](https://doi.org/10.1016/S0043-1354(00)00225-6)

452 Brennan, R.B., Healy, M.G., Morrison, L., Hynes, S., Norton, D., Clifford, E., 2016.
453 Management of landfill leachate: The legacy of European Union Directives. *Waste*
454 *Manag.* 55, 355–363. <https://doi.org/10.1016/j.wasman.2015.10.010>

455 Calabrò, P.S., Scaffoni, S., Orsi, S., Gentili, E., Meoni, C., 2010. The landfill reinjection of
456 concentrated leachate: Findings from a monitoring study at an Italian site. *J. Hazard.*
457 *Mater.* 181, 962–968. <https://doi.org/10.1016/j.jhazmat.2010.05.107>

458 Cingolani, D., Eusebi, A.L., Battistoni, P., 2017. Osmosis process for leachate treatment in
459 industrial platform: Economic and performances evaluations to zero liquid discharge. *J.*
460 *Environ. Manage.* 203, 782–790. <https://doi.org/10.1016/j.jenvman.2016.05.012>

461 Eurostat, 2015. Eurostat: the statistical office of the European Union situated in Luxembourg.
462 http://ec.europa.eu/eurostat/statistics-explained/index.php/Municipal_waste_statistics

463 Eusebi, A.L., Troiani, C., Fatone, F., Battistoni, P., 2009. Biological nitrogen removal at high
464 performances in platform for the treatment of industrial liquid wastes. *Chem. Eng. Trans.*
465 17, 239–244. <https://doi.org/10.3303/CET0917041>

466 Gong, H., Yan, Z., Liang, K.Q.Q., Jin, Z.Y.Y., Wang, K.J.J., 2013. Concentrating process of
467 liquid digestate by disk tube-reverse osmosis system. *Desalination* 326, 30–36.
468 <https://doi.org/10.1016/j.desal.2013.07.010>

469 Hasar, H., Unsal, S.A., Ipek, U., Karatas, S., Cinar, O., Yaman, C., Kinaci, C., 2009.
470 Stripping/flocculation/membrane bioreactor/reverse osmosis treatment of municipal

471 landfill leachate. *J. Hazard. Mater.* 171, 309–317.
472 <https://doi.org/10.1016/j.jhazmat.2009.06.003>

473 Hilal, N., Kim, G.J., Somerfield, C., 2011. Boron removal from saline water: A
474 comprehensive review. *Desalination*. <https://doi.org/10.1016/j.desal.2010.05.012>

475 Insel, G., Dagdar, M., Dogruel, S., Dizge, N., Ubay Cokgor, E., Keskinler, B., 2013.
476 Biodegradation characteristics and size fractionation of landfill leachate for integrated
477 membrane treatment. *J. Hazard. Mater.* 260, 825–832.
478 <https://doi.org/10.1016/J.JHAZMAT.2013.06.037>

479 Joo, S.H., Tansel, B., 2015. Novel technologies for reverse osmosis concentrate treatment: A
480 review. *J. Environ. Manage.* 150, 322–335.
481 <https://doi.org/10.1016/j.jenvman.2014.10.027>

482 Judd, S.J., 2017. Membrane technology costs and me. *Water Res.*
483 <https://doi.org/10.1016/j.watres.2017.05.027>

484 Kim, S., Hoek, E.M.V., 2005. Modeling concentration polarization in reverse osmosis
485 processes. *Desalination* 186, 111–128. <https://doi.org/10.1016/j.desal.2005.05.017>

486 Kuusik, A., Pachel, K., Kuusik, A., Loigu, E., Tang, W.Z., 2014. Reverse osmosis and
487 nanofiltration of biologically treated leachate. *Environ. Technol.* 35, 2416–2426.
488 <https://doi.org/10.1080/09593330.2014.908241>

489 Le, N.L., Nunes, S.P., 2016. Materials and membrane technologies for water and energy
490 sustainability. *Sustain. Mater. Technol.* <https://doi.org/10.1016/j.susmat.2016.02.001>

491 Lee, K.P., Arnot, T.C., Mattia, D., 2011. A review of reverse osmosis membrane materials for
492 desalination-Development to date and future potential. *J. Memb. Sci.*
493 <https://doi.org/10.1016/j.memsci.2010.12.036>

494 Li, F., Wichmann, K., Heine, W., 2009. Treatment of the methanogenic landfill leachate with
495 thin open channel reverse osmosis membrane modules. *Waste Manag.* 29, 960–964.

496 <https://doi.org/10.1016/j.wasman.2008.06.012>

497 Linde, K., Jönsson, A., Wimmerstedt, R., 1995. Treatment of three types of landfill leachate
498 with reverse osmosis. *Desalination* 101, 21–30. <https://doi.org/10.1016/0011->
499 [9164\(95\)00004-L](https://doi.org/10.1016/0011-9164(95)00004-L)

500 Liu, Y., Li, X., Wang, B., Liu, S., 2008. Performance of landfill leachate treatment system
501 with disc-tube reverse osmosis units. *Front. Environ. Sci. Eng. China* 2, 24–31.
502 <https://doi.org/10.1007/s11783-008-0024-x>

503 Mukherjee, S., Mukhopadhyay, S., Hashim, M.A., Sen Gupta, B., 2015. Contemporary
504 Environmental Issues of Landfill Leachate: Assessment and Remedies. *Crit. Rev.*
505 *Environ. Sci. Technol.* 45, 472–590. <https://doi.org/10.1080/10643389.2013.876524>

506 Pérez-González, A., Urtiaga, A.M., Ibáñez, R., Ortiz, I., 2012. State of the art and review on
507 the treatment technologies of water reverse osmosis concentrates. *Water Res.* 46, 267–
508 283. <https://doi.org/10.1016/j.watres.2011.10.046>

509 Peters, T.A., 2001. High advanced open channel membrane desalination (disc tube module).
510 *Desalination* 134, 213–219. [https://doi.org/10.1016/S0011-9164\(01\)00128-X](https://doi.org/10.1016/S0011-9164(01)00128-X)

511 Peters, T.A., 1998. Purification of landfill leachate with reverse osmosis and nanofiltration.
512 *Desalination* 119, 289–293. [https://doi.org/10.1016/S0011-9164\(98\)00171-4](https://doi.org/10.1016/S0011-9164(98)00171-4)

513 Rautenbach, R., Linn, T., 1996. High-pressure reverse osmosis and nanofiltration, a “zero
514 discharge” process combination for the treatment of waste water with severe
515 fouling/scaling potential. *Desalination* 105, 63–70. <https://doi.org/10.1016/0011->
516 [9164\(96\)00059-8](https://doi.org/10.1016/0011-9164(96)00059-8)

517 Renou, S., Givaudan, J.G., Poulain, S., Dirassouyan, F., Moulin, P., 2008. Landfill leachate
518 treatment: Review and opportunity. *J. Hazard. Mater.* 150, 468–493.
519 <https://doi.org/10.1016/j.jhazmat.2007.09.077>

520 Sassi, K.M., Mujtaba, I.M., 2012. Effective design of reverse osmosis based desalination

521 process considering wide range of salinity and seawater temperature. *Desalination* 306,
522 8–16. <https://doi.org/10.1016/j.desal.2012.08.007>

523 Singh, R., 2015. Chapter 1 - Introduction to Membrane Technology, *Membrane Technology*
524 *and Engineering for Water Purification (Second Edition)*.
525 [doi:http://dx.doi.org/10.1016/B978-0-444-63362-0.00001-X](http://dx.doi.org/10.1016/B978-0-444-63362-0.00001-X)

526 Smol, M., Włodarczyk-Makula, M., 2016. Effectiveness in the Removal of Organic
527 Compounds from Municipal Landfill Leachate in Integrated Membrane Systems:
528 Coagulation – NF/RO. *Polycycl. Aromat. Compd.* 1–19.
529 <https://doi.org/10.1080/10406638.2016.1138971>

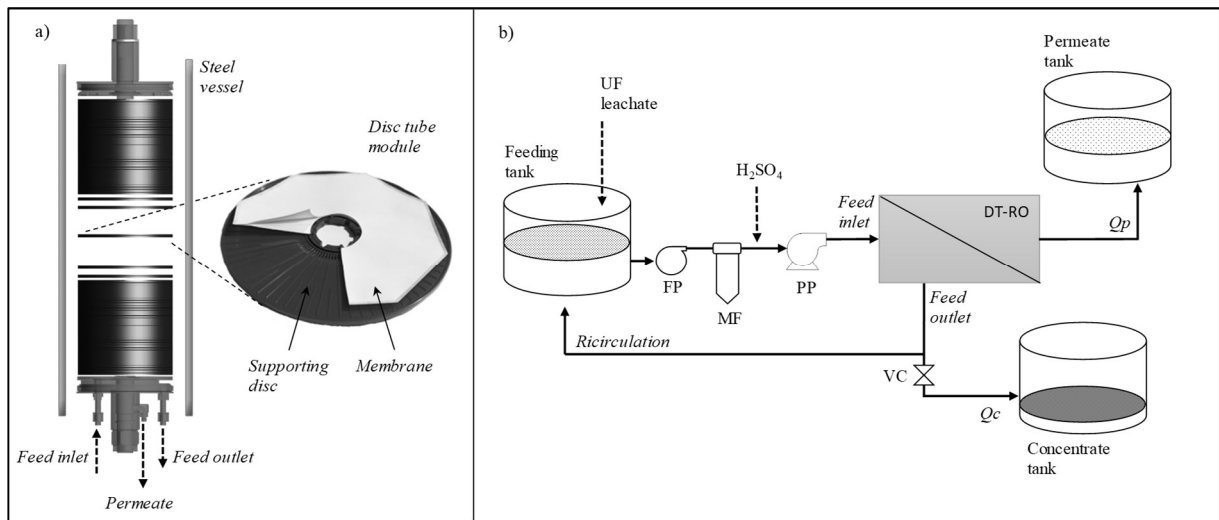
530 Subramani, A., Jacangelo, J.G., 2014. Treatment technologies for reverse osmosis concentrate
531 volume minimization: A review. *Sep. Purif. Technol.*
532 <https://doi.org/10.1016/j.seppur.2013.12.004>

533 Talalaj, I.A., 2015. Removal of organic and inorganic compounds from landfill leachate using
534 reverse osmosis. *Int. J. Environ. Sci. Technol.* 12, 2791–2800.
535 <https://doi.org/10.1007/s13762-014-0661-5>

536 Wijmans, J.G., Baker, R.W., 1995. The solution-diffusion model: a review. *J. Memb. Sci.*
537 107, 1–21. [https://doi.org/10.1016/0376-7388\(95\)00102-I](https://doi.org/10.1016/0376-7388(95)00102-I)

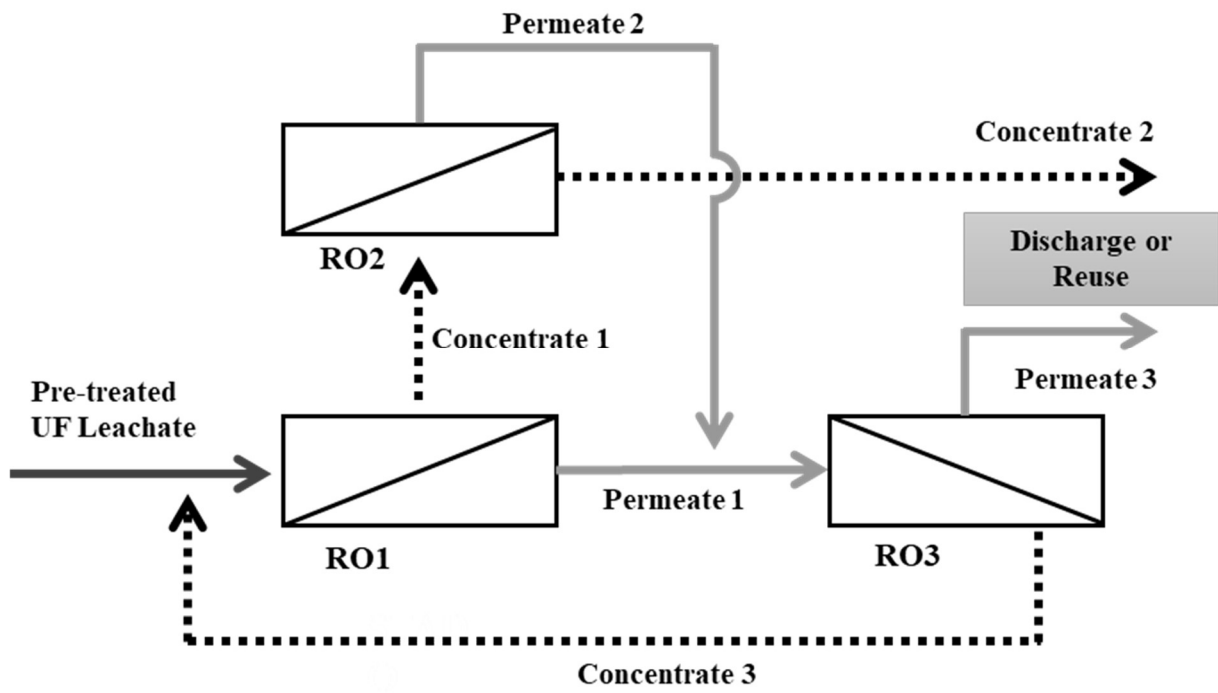
538 Zhang, G., Qin, L., Meng, Q., Fan, Z., Wu, D., 2013. Aerobic SBR/reverse osmosis system
539 enhanced by Fenton oxidation for advanced treatment of old municipal landfill leachate.
540 *Bioresour. Technol.* 142, 261–268. <https://doi.org/10.1016/j.biortech.2013.05.006>

541 Zhao, J., Lu, X.-Q., Luo, J.-H., Liu, J.-Y., Xu, Y.-F., Zhao, A.-H., Liu, F., Tai, J., Qian, G.-R.,
542 Peng, B., 2013. Characterization of fresh leachate from a refuse transfer station under
543 different seasons. *Int. Biodeterior. Biodegradation* 85, 631–637.
544 <https://doi.org/10.1016/j.ibiod.2013.05.012>



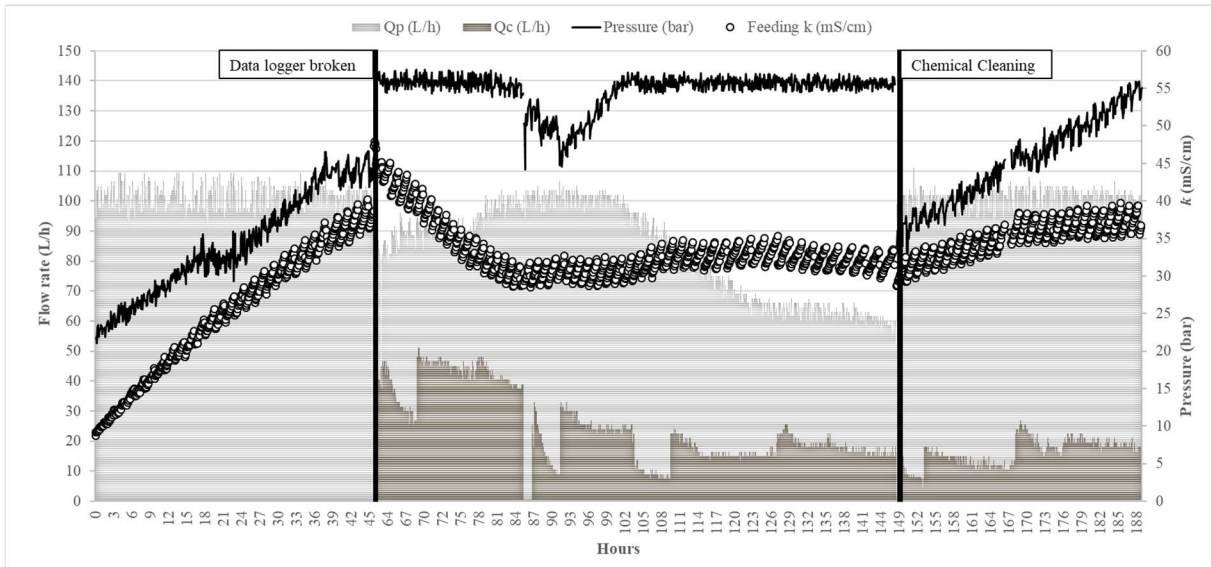
545

546 **Figure 1** DT-RO system (a) and pilot plant flow scheme in RO1 configuration (b).



547

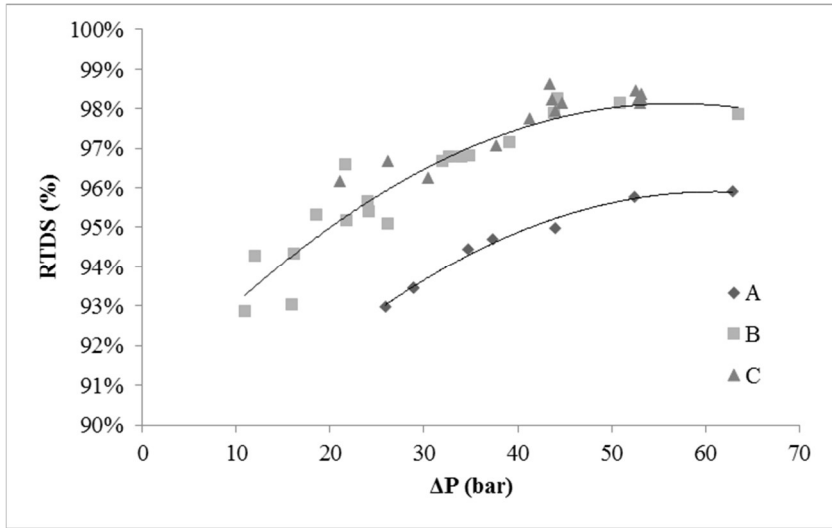
548 **Figure 2** Scheme of the multi-stage treatment by RO membranes.



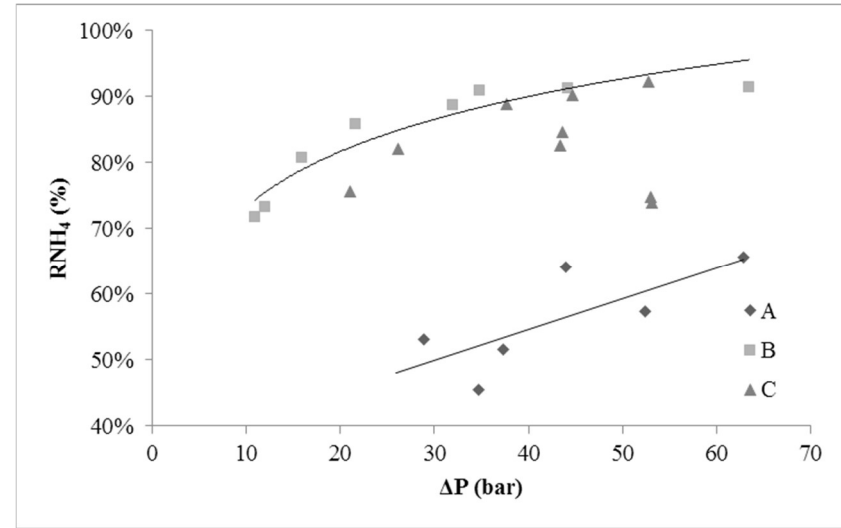
549

550 **Figure 3** RO1_C run: flow rates of permeate (Q_p) and concentrate (Q_c), operative pressure and

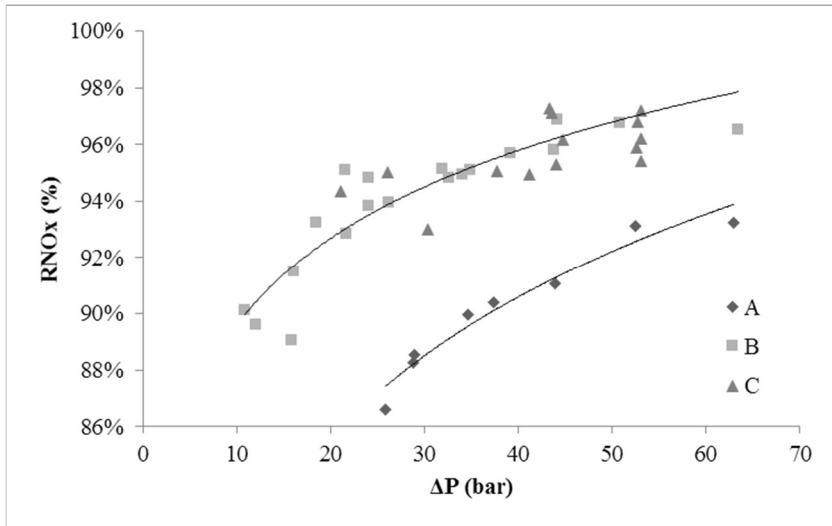
551 electrical conductivity (k) of the feeding.



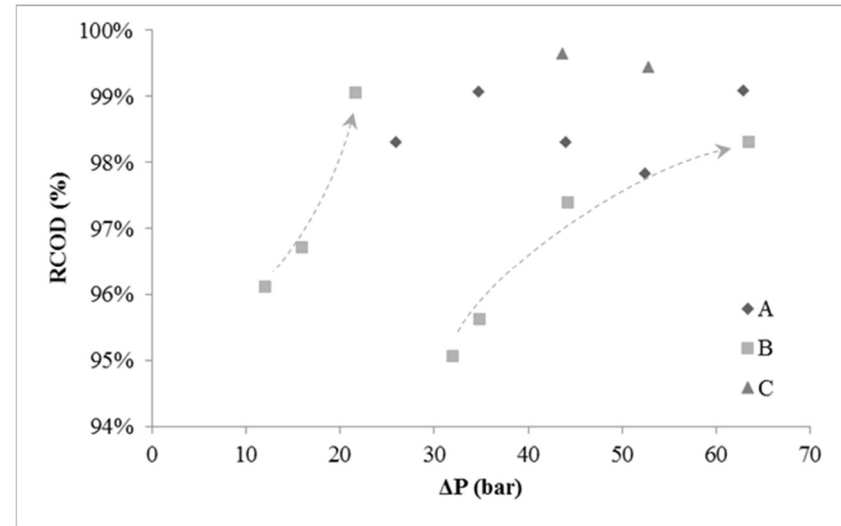
-a Rejection factor for TDS



-b Rejection factor for NH₄

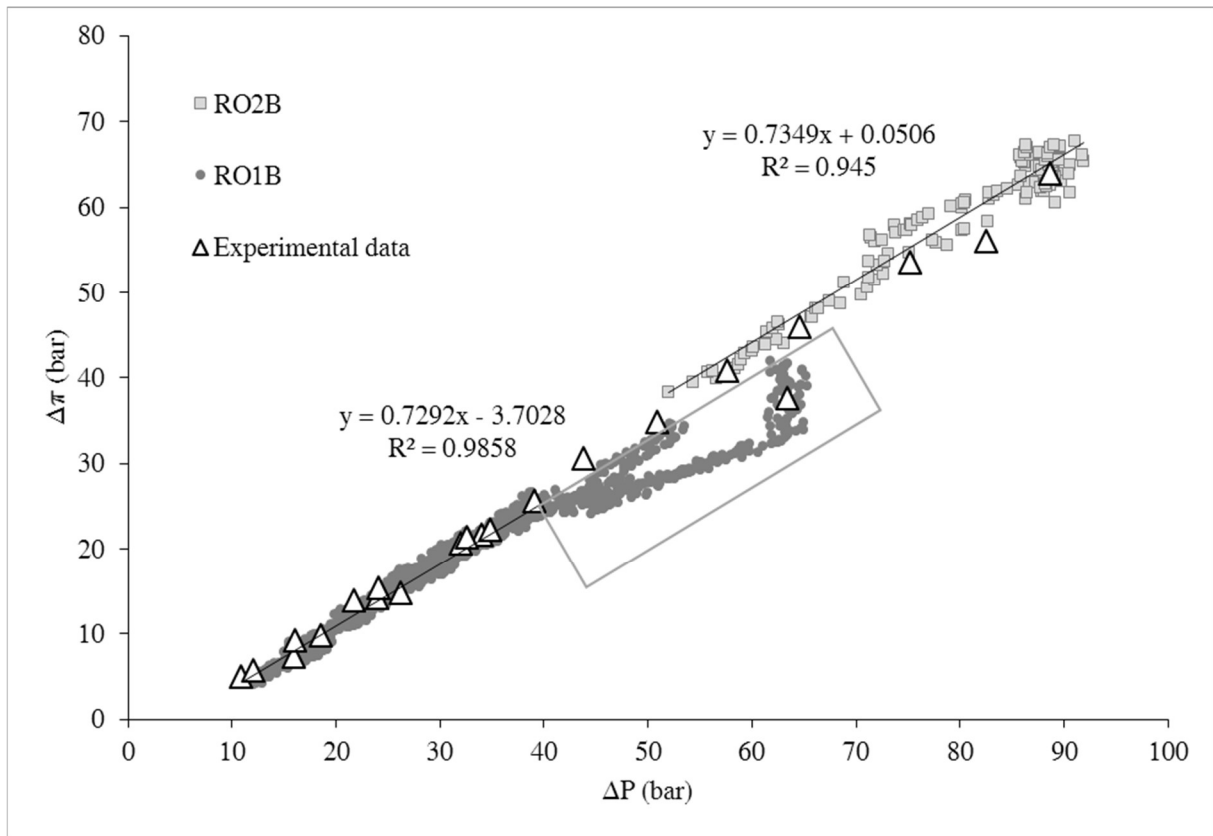


-c Rejection factor for NO_x



-d Rejection factor for COD

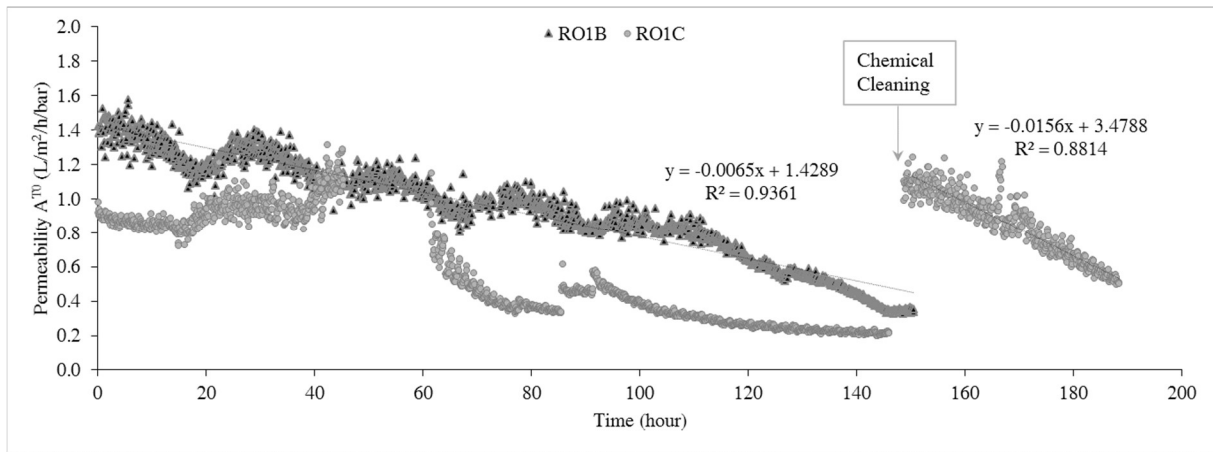
552 **Figure 4** Rejection factors for TDS, NH₄, NO_x and COD observed in RO1 runs (A, B and C).



553

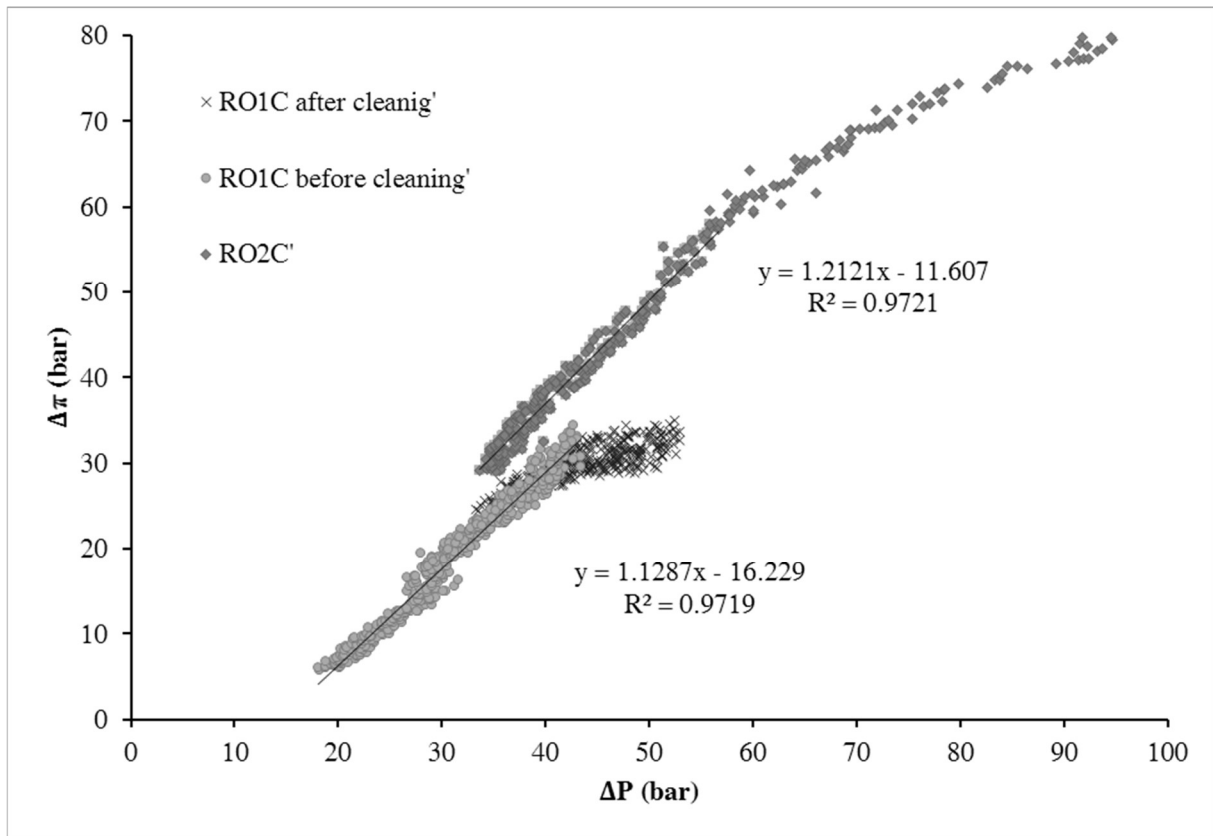
554 **Figure 5** Osmotic pressure differential ($\Delta\pi$) and operative pressure (ΔP) relationship:

555 experimental and modeling data in RO1_B and RO2_B runs.



556

557 **Figure 6** Membrane permeability (A^{T0}) decline in RO1_{B-C} runs.



558

559 **Figure 7** Osmotic pressure differential ($\Delta\pi$) and operative pressure (ΔP) relationship in RO1_C

560 and RO2_C runs (modeling data).

561 **Table 1** Operative parameters of permeate flow rate (Q_p) and flux (J_w), maximum pressure
562 (P_{max}) and temperature.

RO stage	T (°C)	Q_p (L h ⁻¹)	J_w (L m ⁻² h ⁻¹)	P_{max} (bar)	Run
RO1	34-36	100	13.0	60 - 67	A, B, C
RO2	29-37	55	7.1	97	A, B, C
RO3	29-31	250	32.5	60	A, B

563

564 **Table 2** Results of characterization from 20 samples of UF leachate (RO1 feeding) over three
 565 months of monitoring and quality of the permeate of each RO stage.

Parameters	u.m.	UF leachate		RO1 permeate	RO2 permeate	RO3 permeate
			CV			
<i>k</i> (25°C)	mS/cm	8.67 ± 1.97	23%	1.1 ± 0.4	4.4 ± 1.0	0.058 ± 0.033
pH	-	7.2 ± 0.4	6%	5.8 ± 0.1	6.7 ± 0.6	6.0 ± 0.5
Alk	mgCaCO ₃ /L	699 ± 437	63%	44.1 ± 4.0	88 ± 30	11.3 ± 7.9
COD	mg/L	1368 ± 422	31%	82 ± 65	155 ± 139	11.5 ± 6.2
NH₄-N	mg/L	35 ± 46	131%	13.0 ± 9.4	31 ± 26	5.5 ± 0.5
TKN	mg/L	104 ± 85	82%	35 ± 25	42 ± 51	5.9 ± 1.0
NO₂-N	mg/L	206 ± 147	71%	39 ± 27	91 ± 79	2.0 ± 1.5
NO₃-N	mg/L	192 ± 135	70%	90 ± 112	115 ± 93	2.8 ± 2.7
PO₄-P	mg/L	7.5 ± 3.3	44%	0.6 ± 0.7	0.6 ± 0.7	0.1 ± 0.2
Cl	mg/L	1925 ± 426	22%	340 ± 260	631 ± 36	5.3 ± 0.4
SO₄	mg/L	133 ± 46	35%	27 ± 27	47 ± 17	0.3 ± 0.1
Na	mg/L	1562 ± 254	16%	266 ± 178	515 ± 100	9.9 ± 2.3
K	mg/L	556 ± 76	14%	118 ± 82	214 ± 31	4.4 ± 2.4
Mg	mg/L	96 ± 20	21%	6.1 ± 5.3	14.7 ± 2.5	0.5 ± 0.3
Ca	mg/L	161 ± 25	16%	13.5 ± 14.8	25.8 ± 4.2	5.7 ± 0.4

566

567 **Table 3** Removal efficiencies of the main macropollutants and relative pressure for each RO
 568 stage.

Run	Average ΔP (bar)	E_{COD} (%)	E_{NH_4-N} (%)	E_{TKN} (%)	E_{NO_x} (%)	E_{TDS} (%)
RO1 _{A-B-C}	33 - 50	95.9 ± 3.0	60.9 ± 13.4	69.4 ± 5.8	86.4 ± 1.9	91.1 ± 1.5
RO2 _A	21	98.7	86.7 ± 12.9	88.4	84.7	88.9
RO2 _{B-C}	67 - 76			94.8	95.4 ± 3.7	97.7 ± 1.1

569

570 **Table 4** Hazardous compounds concentration in feeding and permeate of RO1, permeate of
 571 RO3 and concentrate of RO2.

(mg/L)	UF leachate		RO1 permeate		RO3 permeate		RO2 concentrate	
	Ave.	St.Dev.	Ave.	St.Dev.	Ave.	St.Dev.	Ave.	St.Dev.
Al	0.319	<i>0.326</i>	0.005	<i>0.002</i>	0.008	<i>0.009</i>	0.925	<i>0.307</i>
Sb	0.017	<i>0.006</i>	0.000	<i>0.000</i>	0.000	<i>0.000</i>	0.098	<i>0.025</i>
As	0.074	<i>0.023</i>	0.002	<i>0.001</i>	0.001	<i>0.000</i>	0.521	<i>0.166</i>
Ba	0.102	<i>0.020</i>	0.017	<i>0.005</i>	0.008	<i>0.001</i>	0.566	<i>0.151</i>
B	5.688	<i>2.549</i>	3.748	<i>0.657</i>	1.950	<i>0.841</i>	16.256	<i>6.524</i>
Cd	0.001	<i>0.000</i>	0.000	<i>0.000</i>	0.002	<i>0.003</i>	0.003	<i>0.001</i>
Cr	0.514	<i>0.175</i>	0.004	<i>0.001</i>	0.002	<i>0.000</i>	6.129	<i>2.906</i>
Fe	2.272	<i>1.265</i>	0.150	<i>0.058</i>	0.169	<i>0.059</i>	13.610	<i>5.675</i>
Mn	0.230	<i>0.175</i>	0.019	<i>0.016</i>	0.004	<i>0.001</i>	1.987	<i>1.379</i>
Hg	0.002	<i>0.001</i>	0.001	<i>0.002</i>	0.000	<i>0.000</i>	0.003	<i>0.001</i>
Ni	0.420	<i>0.164</i>	0.002	<i>0.000</i>	0.001	<i>0.001</i>	3.422	<i>1.115</i>
Pb	0.012	<i>0.005</i>	0.001	<i>0.000</i>	0.000	<i>0.000</i>	0.044	<i>0.004</i>
Cu	0.119	<i>0.046</i>	0.007	<i>0.003</i>	0.003	<i>0.001</i>	0.908	<i>0.189</i>
Se	0.063	<i>0.036</i>	0.004	<i>0.002</i>	0.000	<i>0.000</i>	0.471	<i>0.204</i>
Sn	0.026	<i>0.007</i>	0.001	<i>0.000</i>	0.001	<i>0.000</i>	0.125	<i>0.040</i>
V	0.131	<i>0.046</i>	0.003	<i>0.001</i>	0.001	<i>0.000</i>	1.004	<i>0.388</i>
Zn	0.680	<i>0.183</i>	0.199	<i>0.066</i>	0.164	<i>0.044</i>	3.214	<i>0.189</i>

572

573 **List of Figures**

574

575 **Figure 1** DT-RO system (a) and pilot plant flow scheme in RO1 configuration (b).

576 **Figure 2** Scheme of the multi-stage treatment by RO membranes.

577 **Figure 3** RO1_C run: flow rates of permeate (Q_p) and concentrate (Q_c), operative pressure and
578 electrical conductivity (k) of the feeding.

579 **Figure 4** Rejection factors for TDS, NH_4 , NO_x and COD observed in RO1 runs (A, B and C).

580 **Figure 5** Osmotic pressure differential ($\Delta\pi$) and operative pressure (ΔP) relationship:
581 experimental and modeling data in RO1_B and RO2_B runs.

582 **Figure 6** Membrane permeability (A^{T0}) decline in RO1_{B-C} runs.

583 **Figure 7** Osmotic pressure differential ($\Delta\pi$) and operative pressure (ΔP) relationship in RO1_C
584 and RO2_C runs (modeling data).

585 **List of Tables**

586

587 **Table 1** Operative parameters of permeate flow rate (Q_p) and flux (J_w), maximum pressure
588 (P_{max}) and temperature.

589 **Table 2** Results of characterization from 20 samples of UF leachate (RO1 feeding) over three
590 months of monitoring and quality of the permeate of each RO stage.

591 **Table 3** Removal efficiencies of the main macropollutants and relative pressure for each RO
592 stage.

593 **Table 4** Hazardous compounds concentration on feeding and permeate of RO1, permeate of
594 RO3 and concentrate of RO2.